American Journal of Transplantation 2014; XX: 1–11
Wiley Periodicals Inc.

doi: 10.1111/ajt.12797

Immunological Status of Isolated Lymphoid Follicles After Intestinal Transplantation

D. Meier[1,*], G. H. Docena[2], D. Ramisch[3], U. Toscanini[4], G. Berardi[4], G. E. Gondolesi[1,3] and M. Rumbo[2]

[1]*Laboratory of Translational Research and Transplant Immunology, Multiorgan Transplantation Institute, Favaloro University, Buenos Aires, Argentina*
[2]*Laboratory of Immunological Research, Faculty of Exact Sciences, National University of La Plata, La Plata, Argentina*
[3]*Nutrition, Rehabilitation, and Intestinal Transplantation Unit, Multiorgan Transplantation Institute, Favaloro Foundation University Hospital, Buenos Aires, Argentina*
[4]*PRICAI, Favaloro Foundation University Hospital, Buenos Aires, Argentina*
[*]*Corresponding author: Dominik Meier, dmeier@ffavaloro.org*

Intestinal transplantation (ITx) faces the challenge of grafting a high immunogenic organ, which is certainly one of the major obstacles for intestinal allograft acceptance. The allograft has to guarantee the proper functioning of the mucosal immune machinery under immunosuppressive conditions. Recently, it has been elucidated that isolated lymphoid follicles (ILFs) are an indispensable part of mucosal immunity to maintain IgA synthesis and consequently to control commensal microflora. No data about these follicular structures in the setting of ITx are available so far. Therefore, we addressed the question whether constitution, integrity and function of allograft ILFs are disturbed by immunosuppressive regimen. We compared allograft ILFs from terminal ileum of transplant patients with ILFs from nontransplant patients via flow cytometry, quantitative real-time polymerase chain reaction and immunohistochemistry. We found that host leukocytes rapidly repopulate allograft ILFs and that maintenance immunosuppressive regimen, tacrolimus and corticosteroids, does not affect their cellular integrity and function. However, allograft ILFs revealed a higher maturation state than control samples and IgA positive plasma cells were increased in number in allograft mucosa. Our results open the path for a better understanding of allograft mucosal immunity.

Abbreviations: ACR, acute cellular rejection; *ACTB*, beta actin; AICDA, activation-induced cytidine deaminase; BCL6, B cell lymphoma 6 protein; Ct, threshold cycles; EDTA, ethylenediamine tetraacetic acid; FITC, fluorescein isothiocyanate; FOXP3, forkhead box P3; GC, germinal center; HBSS, Hank's Balanced Salt solution; ILF, isolated lymphoid follicle; ITx, intestinal transplantation; LP, lamina propria; MMF, mycophenolate mofetil; PCR, polymerase chain reaction; PD-1, programmed cell death-1; PE, phycoerythrin; PP, Peyer's patch; RORC, RAR-related orphan receptor C; RT, room temperature; SEM, standard error of the mean; SHM, somatic hypermutation; STR, short tandem repeat; T_{FH}, follicular helper T cells; TGFB, transforming growth factor beta; Th, T helper; Treg, regulatory T cell; Tx, transplant

Received 02 December 2013, revised 20 March 2014 and accepted for publication 17 April 2014

Introduction

Intestinal transplantation (ITx) is a well-accepted treatment for intestinal failure and life-threatening complications of chronic parenteral nutrition (1). Graft loss, secondary to acute cellular rejection (ACR) and infection episodes, is still an unresolved problem and is more prominent in ITx than in other solid organ transplantation (2). The reason for this discrepancy in graft loss might be found in the particularity of the small bowel: a large absorptive surface area, which is in permanent contact to foreign antigens of commensals, food and pathogens, consequently bearing a high number of immune cells (3). The small bowel allograft has to assure functionality of mucosal immune machinery after transplant operation concomitant with suppression of an allo-reactive immune response.

Isolated lymphoid follicles (ILFs), also referred to as solitary lymphoid follicles (4,5), are part of this mucosal immune machinery (6–9) and can be clearly distinguished from Peyer's patches (PPs) (10,11). Mature ILFs contain a germinal center (GC) with mainly follicular B-lymphocytes (12), $CD4^+$ follicular helper T cells (T_{FH}) (13) and follicular dendritic cells (14). These small lymphoid structures seated all over the small bowel are highly dynamic serving as an important inductive site for IgA synthesis confronting changes in the microbiota (15,16). ILF hyperplasia and uncontrolled growth of commensals were shown in an activation-induced cytidine deaminase (AICDA) null mice, where class switch recombination and somatic hypermutation (SHM) are inhibited (17), whereas reduced number of ILFs were detected in antibiotic-treated or in germ-free mice (18,19). Little is known about human ILFs in general

and to our knowledge, no studies of ILFs from the intestinal allograft have been reported. Therefore, we wanted to address the question whether constitution, integrity and functional properties of allograft ILFs are affected after ITx by the chronic use of immunosuppressive regimen.

A unique feature of ITx is the presence of a surgically created ileostomy, which serves as an access for endoscopic graft surveillance. After several months without any sign of clinical complications, the ileostomy closure surgery is conducted. We decided to examine the allograft ILFs from the tissue specimen of ileostomy closure and compared them with nonpathogenic, nontransplanted ILFs. We show that immunosuppressive regimen is not significantly influencing cell composition within ILFs, although allograft ILFs had a higher maturation state compared to control ILFs. In addition, we characterized $CD4^+$ T helper (Th) cell subsets of ILFs and analyzed cell repopulation of allograft ILFs. This study opens the path for a better understanding of allograft mucosal immunity.

Materials and Methods

Patients and study groups

Details of ITx surgical procedures, immunosuppressive therapy and patients' follow-up care were previously reported (20,21). Two different study groups were used. The first group, referred to as transplant (Tx) or allograft group, contained eight patients (five children and three adults). Tissue specimens from patients of this group were obtained either from tissue biopsies of routine endoscopic surveillance (6–12 days post-ITx) or from ileostomy closure operation (between 289 and 1085 days post-ITx). Tx patient data are summarized in Table 1a. Histological evaluations of biopsy specimens were conducted by trained pathologists using the classical rejection grading system (22). The second group (non-Tx group) included samples obtained from 10 non-Tx patients (two children and eight adults) undergoing other abdominal surgical procedures from which a distal ileum segment was obtained and used as healthy control group (Table 1b). None of the samples obtained were from infected, inflamed, or neoplastic tissue. Informed consent was approved by the institutional ethic committee and IRB (DDI [1125] 511) was obtained.

Isolation of human isolated lymphoid follicles

After ileal resection, specimen was washed in Hank's Balanced Salt solution (HBSS; Life Technologies, Carlsbad, CA), and seromuscular layer removed by dissecting throughout submucosal layer. The remaining mucosal layer was incubated in HBSS containing 20 mM ethylenediamine tetraacetic acid (EDTA; Sigma, St. Louis, MO) and 100 U/mL penicillin-streptomycin (Sigma) for 20 min at room temperature (RT) on a shaker. Next, tissue specimen was washed with HBSS by vortexing roughly five times for 30 s each. The remaining tissue was then observed under a stereomicroscope to identify, count, and isolate ILFs. Isolated ILFs were pooled and homogenized either for flow cytometry analysis in 0.5 mL Dulbecco's phosphate-buffered saline (Sigma) containing 2% fetal bovine serum (PAA, Pasching, Austria), or for RNA isolation in RA1 lysis buffer (GE Healthcare, Little Chalfont, UK).

Table 1a: ITx patient data on age, gender, donor, time of ileostomy closure and immunosuppressive regimen

Patient	Age/gender	Donor age/gender	Time until closure (days)	Immunosuppression				
				Induction	Maintenance			Major changes
1	23/M	18/M	471	Basiliximab	FK506	Cort	MMF	No
2	12/M	14/M	454	Basiliximab	FK506	Cort	MMF	MMF *wo*, 272 dpic
3	1.4/M	4/F	429	Basiliximab	FK506	Cort	MMF	MMF *wo*, 366 dpic
4	2/M	14/F	396	Basiliximab	FK506	Cort	MMF	MMF *wo*, 392 dpic; Rapa *wo*, 196 dpic
5	10/F	8/F	582	Thymo	FK506	Cort	No	No
6	9/M	5/F	1085	Thymo	FK506	Cort	MMF	MMF *wo*, 909 dpic
7	55/F	29/F	370	Basiliximab	FK506	Cort	MMF	MMF *wo*, 33 dpic, Rapa *wo*, 280 dpic
8	21/M	18/M	289	Basiliximab	FK506	Cort	MMF	MMF *wo*, 57 dpic

ITx patient data on type, underlying disease, ACR episodes and viral infection

Patient	Type	Underlying disease	ACR episodes at days preileostomy closure			Viral infection at dpic
1	Isolated	Sepsis abdominal	Mild 1: 360	Mild 2: 233		No
2	Isolated	Gastroschisis	No			Cytomegalovirus: 406
3	Combined	Nec. enterocolitis	Mild: 418			No
4	Isolated	Volvulus	Severe: 376	Mild: 360		No
5	Isolated	Volvulus	Severe: 552	Mild 1: 556	Mild 2: 327	Rotavirus: 298; Noro: 182
6	Isolated	Volvulus	Mild: 519			Adenovirus: 180
7	Isolated	Ischemia	Mild: 264			No
8	Isolated	Trauma	No			No

Histological report of ileostomy closure sample: Histological examination of hematoxylin and eosin sections of all samples resulted as follows: normal aspect of villosity; preserved crypts; lamina propria with some view inflammatory lymphoplasmacytic infiltrates; follicles with reactive germinal centers.

ACR, acute cellular rejection; Cort, corticosteroid; dpic, days preileostomy closure; FK506, tacrolimus; ITx, intestinal transplantation; MMF, mycophenolate mofetil; Nec., necrotizing; Rapa, rapamycin; Thymo, thymoglobulin; *wo*, weaned off immunosuppression.

Table 1b: Nontransplant patient data on age, gender and tissue specimen

Patient	Age	Gender	Origin of tissue specimen
9	Adult	F	Transplant (donor)
10	7	F	Cystic lymphangioma
11	59	F	Right hemicolectomy
12	20	M	Transplant (donor)
13	22	M	Transplant (donor)
14	18	M	Transplant (donor)
15	Adult	M	Transplant (donor)
16	15	M	Transplant (donor)
17	55	M	Autologous GI reconstruction
18	52	M	Right hemicolectomy

Histological report: Histological examination of hematoxylin and eosin sections of all nontransplant samples resulted as follows: normal aspect of villosity; preserved crypts; lamina propria without inflammatory cells; follicles within the normal range.
M, male; F, female.

Flow cytometry

The mAbs that were used for cell staining are listed in Table 2. mAbs were added to the cells and incubated for 20 min at RT in the dark. Cells were washed, resuspended in Dulbecco's phosphate-buffered saline, and analyzed by flow cytometry (FACS Calibur, BD Biosciences). Data was analyzed by FlowJo software (Tree Star, Ashland, OR).

Immunohistochemistry

Tissue specimens were fixed in buffered 10% formalin, paraffin-embedded and 4 μm tissue sections were mounted on Superfrost Plus microscope slides (BioGenex, Fremont, CA). Sections were incubated at 60°C for 1 h, deparaffinized, rehydrated and antigen retrieval were performed in citrate buffer pH 6.0 (BioGenex) by microwave heating for 15 min. Sections were further incubated with peroxide blocking solution (BioGenex) and subsequently with normal goat serum blocking solution (BioGenex), 15 min each. Primary antibodies used are listed in Table 2. Primary antibody was incubated for 1 h at RT followed by the use of multilink-HRP detection system (BioGenex) with 3-amino-9-ethylcarbazol. Finally, sections were counterstained with hematoxylin and mounted with aqueous mounting media (BioGenex).

RNA isolation and cDNA synthesis

Isolation of RNA from homogenized ILF and lamina propria (LP) tissue was conducted by manufacturer's manual of the RNAspin mini isolation kit (GE Healthcare). RNA concentration was measured by NanoDrop spectrophotometer (Thermo Fisher Scientific, Waltham, MA). Five hundred nanograms of total RNA was applied for cDNA synthesis, which was performed according to the MMVL reverse transcriptase kit instructions (Life Technologies).

Quantitative real-time polymerase chain reaction

Expression levels of mRNA were quantified by real-time polymerase chain reaction (PCR) with SYBR®GreenER™ quantitative PCR SuperMix for iCycler® (BioRad, Hercules, CA). Primer sequences are listed in Table 2. PCR consisted of a 10 min at 95°C denaturation step followed by 40 cycles of an annealing and extension step at 60°C for 1 min and a denaturation step at 95°C for 15 s. Nontemplate controls for each primer pair were performed. Gene quantification was calculated using the number of threshold cycles (Ct) and the ΔΔCt method with beta actin (*ACTB*) as housekeeping gene (23).

Laser dissection microscopy and genomic DNA isolation

Paraffin sections of thickness 8 μm were placed on PEN-membrane coated slides (Leica, Wetzlar, Germany), incubated at 60°C for 1 h, deparaffinized,

Table 2: Antibodies and primer sequences used in this study

Antibody	Fluorescence	Clone	Assay	Manufacturer
CD3	PECy5	HIT3a	FACS	BD Biosciences
CD4	PE	RPA-T4	FACS	BD Biosciences
CD8	APC	HIT8a	FACS	BD Biosciences
CD19	FITC	HIB19	FACS	BD Biosciences
CD56	FITC	NCAM16.2	FACS	BD Biosciences
CD69	FITC	FN50	FACS	BD Biosciences
CXCR5	FITC	RF8B2	FACS	BD Biosciences
CCR6	PE	11A9	FACS	BD Biosciences
AICDA		ZA001	IHC	Life Technologies
Ki-67		EPR3611	IHC	BioGenex
CD57		HNK-1	IHC	BD Biosciences
PD-1		MIH4	IHC	BD Biosciences
IgA	Biotin	Polyclonal	IHC	Life Technologies

Primer	5′-Sequence (5′–3′)	3′-Sequence (5′–3′)
ACTB	CCTGGCAC CCAGCACAAT	GCCGATCCACACGGAGTACT
AICDA	TCCTTTTCACTGGACTTTGGTTATC	TGTAGCG GAGGAAGAGCAATTC
BCL6	CCAACCTGAAAACCCACACT	TGTGACGGAAATGCAGGTTA
CXCL13	GACGCTTCATTGATCGAATTCA	TTCCAGACTATGATTTCTTTTCTTGG
FOXP3	CATGATCAGCCTCACACCAC	CCACTTGCAGACACCATTTG
IL17A	CCTCAGATTACTACAACCGA	GACACCAGTATCTTCTCCAG
IL21	TGTGAATGACTTGGTCCCTGAA	AGCAGGAAAAAGCTGACCACTCA
RORC	TGGAGCTGGCCTTTCATCA	GCTACACAGGCTCCGAAGCTT
TGFB	CCCACAACGA AATCTATGAC	CTGTATTTCTGGTACAGCTC

ACTB, beta actin; APC, allophycocyanin; CD, cluster of differentiation; FACS, fluorescence-activated cell sorting; FITC, fluorescein isothiocyanate; IHC, immunohistochemistry; PE, phycoerythrin.

hydrated and dried for 30 min at 50°C. Then, ILFs were identified under a laser dissection microscope, model LMD6500 (Leica), cut out and captured in a 0.2 mL PCR tube containing lysis buffer from RecoverAll™ total nucleic acid isolation kit (Life Technologies). Subsequently, genomic DNA isolation was performed according to manufacturer's instructions of RecoverAll™ total nucleic acid isolation kit.

Short tandem repeat analysis

To estimate percentage of donor versus recipient tissue within ILFs, short tandem repeat (STR) analysis was performed by AmpFISTR® MiniFiler™ or Identifiler® PCR amplification kit (Applied Biosystems, Carlsbad, CA). PCR amplification was performed using GeneAmp® PCR System 9700 (Applied Biosystems). GeneMapper® ID version 3.2 software (Applied Biosystems) was used for allele discrimination. The percentage of each single allele peak height compared to the peak height of individual recipient and donor samples and, subsequently, mean of these percentages (4–11 peaks/sample) were calculated.

Statistical analysis

Results are expressed as mean and standard error of the mean (SEM). Statistical analysis was performed using unpaired Student's *t*-test and one-way analysis of variance with a significance level of $p < 0.05$.

Results

Identification of isolated lymphoid follicles in human allograft tissue

In human tissue, discrimination of ILFs and PPs is complex because PPs are variable in size along the small bowel and follicular structures are not easily visible by the eye (Figure 1A). PPs are defined as clusters of three or more follicles (24,25). We established a protocol to discriminate ILFs from PPs in human tissue for isolating follicular structures containing only one follicle (Figure 1B). The procedure includes manual dissection of mucosa (Figure 1C) and serial EDTA incubation/washing to detach mucus and the epithelial layer (Figure 1D), resulting in a high visibility of follicular structures to clearly distinguish ILFs.

Tissue obtained during the ileostomy closure (Figure 1E) is the optimal sample to study allograft ILFs, as the distal ileum has the highest incidence of follicular structures (24,25) and the ileostomy closure operation permit obtaining an important amount of material. We obtained tissue specimen with a mean size of 9.8 ± 6.8 cm of distal ileum and the surface area after dissection was 24.4 ± 11 cm^2 with a mean of 2.5 ± 1.5 ILFs/cm^2 (Figure 1F). The tissue specimen obtained from the healthy control group had a mean size of 5.5 ± 1.4 cm, the ILF-counting surface area had a mean of 15.9 ± 7.5 cm^2, and the non-Tx ILF number was slightly, but not significantly, decreased compared to the allograft tissue (1.8 ± 0.8 ILFs/cm^2; $p = 0.326$).

Recipient leukocytes repopulate allograft isolated lymphoid follicles

Next, we investigated whether ILFs are repopulated early by recipient cells and whether donor follicular cells persist in the long term. We selected paraffin-embedded biopsies containing ILF structures at early days post-ITx and compared them with ILFs identified at ileostomy closure by performing a donor-recipient genomic DNA analysis cutting out ILFs by laser dissection microscopy (Figure 2A). In the biopsies from the first week post-Tx, on average $37 \pm 10.9\%$ of the follicular cells were of host origin, whereas at the closure time $88.2 \pm 10\%$ of ILF tissue was of host origin (Figure 2B).

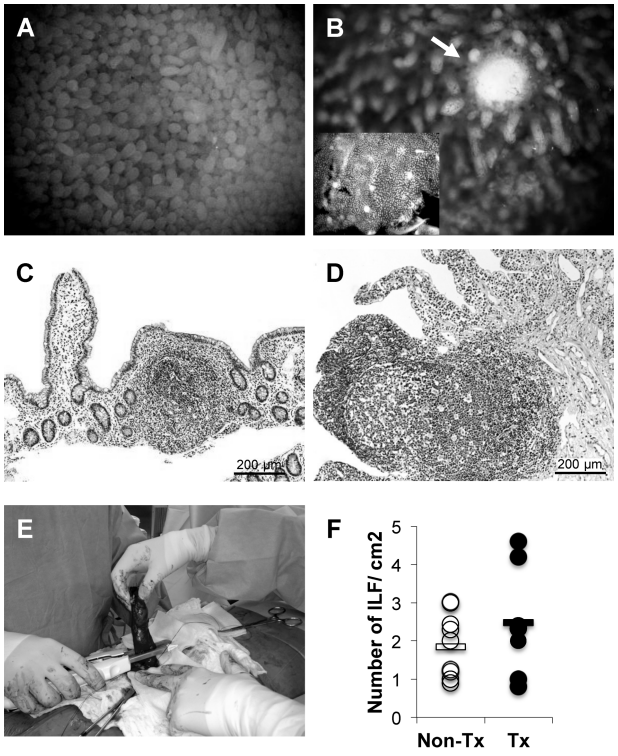

Figure 1: Identification and collection of isolated lymphoid follicles (ILF) from allograft intestine. (A) Representative picture of distal ileum from the luminal site. (B) Identification of ILF (arrow) after a complete washing out of epithelial monolayer. Inset showing (with lower magnification) the distribution of ILFs in a distal ileum tissue without epithelium and seromuscular layer. (C) Hematoxylin and eosin of representative tissue slide of ILF with epithelial monolayer before ethylenediamine tetraacetic acid (EDTA) treatment and (D) ILF after EDTA treatment without epithelium. (E) Photo illustrating partition of tissue specimen at operation of ileostomy closure. (F) Number of ILFs/cm^2 mucosal tissue from nontransplant ($N = 10$) and allograft samples ($N = 8$). Circle represents individual samples and bar represents mean.

Immunosuppressive regimen does not affect lymphocytes in allograft isolated lymphoid follicles

Next, we studied the cellularity of ILFs by flow cytometry from allograft and non-Tx tissue. We counted a slightly higher cell number in allograft ILFs than in non-Tx ILFs ($1.05 \times 10^5 \pm 0.19$ cells of seven non-Tx vs. $1.15 \times 10^5 \pm 0.19$ cells in five Tx, $p = 0.352$). The mean numbers of relative percentages of CD19$^+$ B cells ($58.6 \pm 5.2\%$ in seven non-Tx vs.

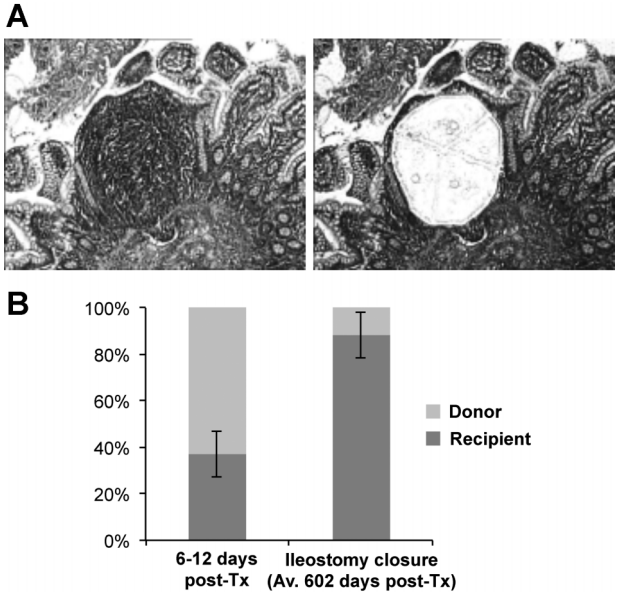

Figure 2: Allograft ILFs of the ileostomy loop are perfectly repopulated by recipient cells. (A) Representative pictures of an ILF from distal ileum sample before (left panel) and after (right panel) laser dissection microscopy for genomic DNA capturing. (B) Bar graph shows donor-recipient cell chimerism of allograft ILFs at an early time point (range: 6–12 days post-ITx; N = 4) and at the time of ileostomy closure (range: 61–155 weeks post-ITx; N = 5). Mean and standard deviation of the calculated mean percentages of the allele peak height of each patient are expressed. ILF, isolated lymphoid follicle; ITx, intestinal transplantation.

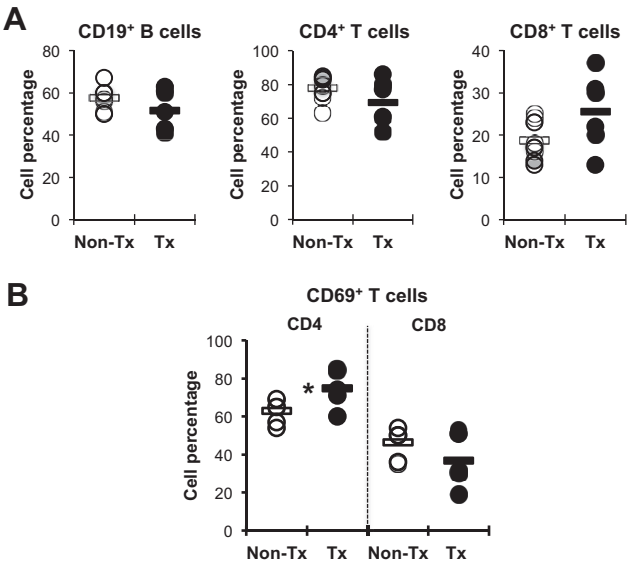

Figure 3: Immunosuppressive regimen does not influence composition of main lymphocyte subsets in allograft isolated lymphoid follicles. (A) Illustration of relative cell percentages of the major lymphocyte populations in the lymphocyte gate from flow cytometric analysis and (B) of $CD69^+$ cells in either the $CD4^+$ or the $CD8^+$ T cells. Each circle representing individual samples and bar representing mean. * indicates significant differences.

$50 \pm 9.6\%$ in six Tx, $p = 0.065$) and $CD3^+$ T cells ($33 \pm 7\%$ vs. $41.6 \pm 9.2\%$, $p = 0.095$), the two main cell types found in ILFs, were not significantly different between allograft and non-Tx ILFs (Figure 3A). We further analyzed within the $CD3^+$ T cell population the percentage of $CD4^+$ T cells ($78.4 \pm 7.6\%$ vs. $72.8 \pm 11.7\%$, $p = 0.334$) and $CD8^+$ T cells ($18 \pm 4.5\%$ vs. $24.4 \pm 9.7\%$, $p = 0.154$) and found no significant differences, although a slight increase of $CD8^+$ T cells ($1.4\times$) in allograft ILFs was found.

In addition, we determined the difference between the expression levels of the T cell activation marker CD69 on $CD4^+$ and $CD8^+$ T cells from non-Tx and allograft ILFs. A slight increase of $CD4^+$ $CD69^+$ T cells in allograft ILFs compared to non-Tx ILFs ($62 \pm 6.2\%$ in five non-Tx vs. $74.8 \pm 10.3\%$ in five Tx samples, $p = 0.045$) was detected, whereas a slight decrease of $CD8^+$ $CD69^+$ T cells in allograft ILFs ($45 \pm 8.8\%$ non-Tx vs. $36.8 \pm 14.7\%$ Tx, $p = 0.266$) was calculated (Figure 3B).

Identification of $CD4^+$ T helper cell subsets in isolated lymphoid follicles

$CD4^+$ T_{FH} are essential for maintenance of GCs and for affinity maturation (13,26). Immunosuppressive regimen, especially calcineurin inhibitors such as tacrolimus, has the capacity to interfere with T_{FH} (27). Therefore, we wanted to elucidate whether T_{FH} located in allograft ILF are hindered by the immunosuppressive regimen. As specific markers, we used two chemokine receptors CXCR5 and CCR6, which are recognized to discriminate T cell subsets (28,29). CXCR5 is highly expressed on T_{FH}, whereas CCR6 is mainly expressed on T helper 17 (Th17) cells and on regulatory T cells (Tregs). We clearly identified for the first time in human ILFs $CXCR5^+$ and $CCR6^+$ $CD4^+$ T cell subsets by flow cytometry in both non-Tx and allograft ILFs (Figure 4A). Quantifications revealed no differences of relative cell percentages between the $CD4^+$ $CXCR5^+$ T cell subsets in non-Tx ($32.4 \pm 4.2\%$; N = 5) and Tx samples ($31.3 \pm 2.1\%$, N = 3; $p = 0.069$), whereas in the $CD4^+$ $CCR6^+$ T cell subsets of non-Tx (18.4 ± 3.8; N = 9) and Tx (12.5 ± 5.9; N = 5) samples, a significant decrease of cell percentages in the allograft ILFs was calculated ($p = 0.041$) (Figure 4B).

By cell sorting of the $CXCR5^+$ and $CCR6^+$ $CD4^+$ T cell subsets and subsequently isolating mRNA, we wanted to elucidate gene expression levels of the crucial transcription factors for Th cell differentiation, namely B cell lymphoma 6 protein (BCL6) for T_{FH}, RAR-related orphan receptor C (RORC) for Th17 cells, and forkhead box P3 (FOXP3) for Tregs. Our results reveal that the $CD4^+$ $CXCR5^+$ T cell subset expresses a sixfold higher increase of *BCL6* mRNA than $CD4^+$ $CCR6^+$ T cell subset, whereas $CCR6^+$ T cells express a 13-fold higher level of *RORC* mRNA and a fivefold higher level of *FOXP3* mRNA than the $CXCR5^+$ T cell subset

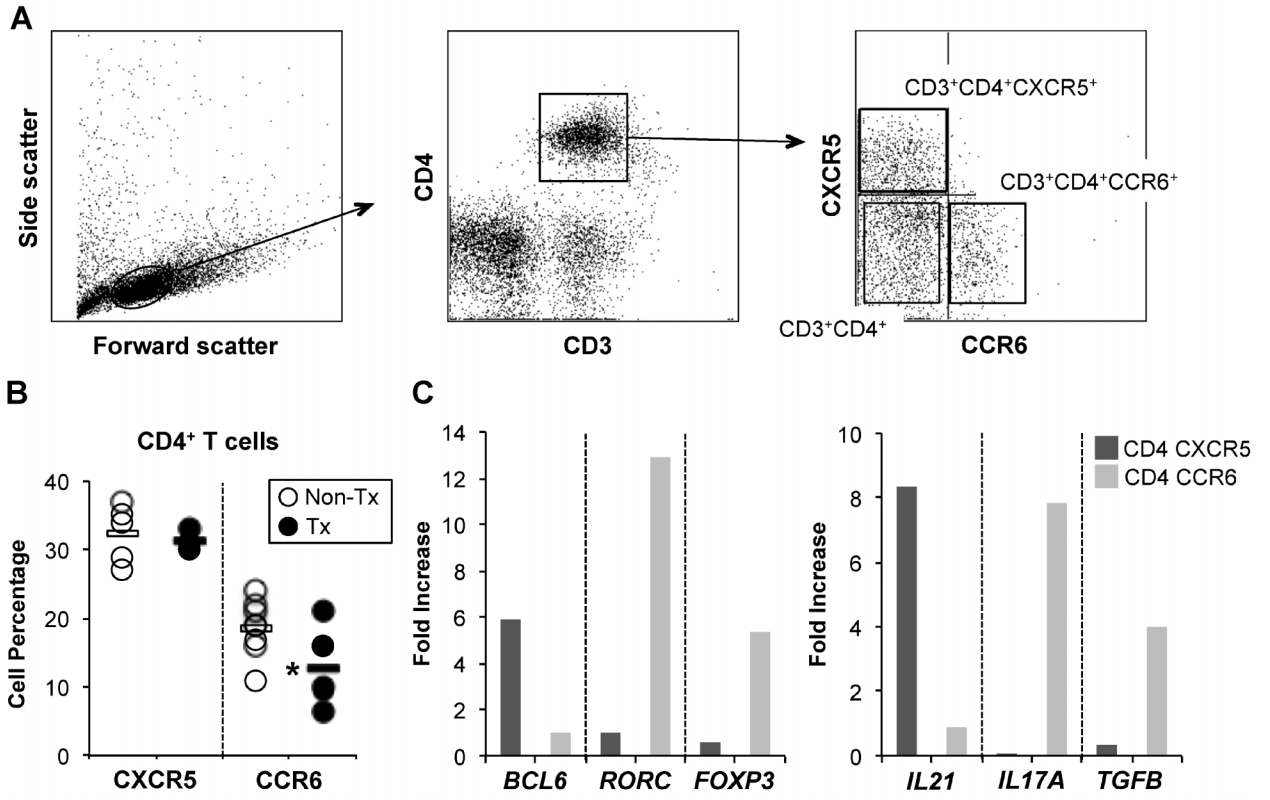

Figure 4: Studies of CD4+ T cell subsets from human isolated lymphoid follicles. (A) Representative dot plots of flow cytometric analysis of isolated lymphoid follicle samples and gating strategy for cell sorting of $CD4^+$ T cell subsets with chemokine receptors resulting in three subsets: $CD3^+$ $CD4^+$ T cells, $CD3^+$ $CD4^+$ $CXCR5^+$ T cells and $CD3^+$ $CD4^+$ $CCR6^+$ T cells. (B) Relative cell percentage of gated $CD4^+$ $CXCR5^+$ T cells and $CD4^+$ $CCR6^+$ T cells. Circle represents individual samples and bar represents mean. (C) Gene expression analysis of indicated genes from $CD4^+$ $CXCR5^+$ and $CD4^+$ $CCR6^+$ T cells. Fold increase represents $\Delta\Delta$Ct method with $CD4^+$ double negative T cells as normalizer. * indicates significant differences. Ct, threshold cycles.

(Figure 4C). In addition, we determined the mRNA expression level of typical cytokines expressed by each T cell subset (IL-21 by T_{FH}; IL-17A by Th17 cells; and transforming growth factor beta [TGFB] by Tregs). We found that the $CXCR5^+$ T cells express eightfold increased level of *IL21* mRNA than $CCR6^+$ T cells, whereas the expression levels of *IL17A* and *TGFB* are eightfold and fourfold increased, respectively in $CCR6^+$ T cells compared to $CXCR5^+$ T cells.

Allograft isolated lymphoid follicles contain hyperactive germinal centers

Next, we wanted to elucidate whether allograft ILFs contain a functional GC and whether the activation state are comparable to non-Tx ILFs. Mature ILFs contain GCs, where clonal B cell expansion and SHM in the so-called dark zone, and class switch recombination in the light zone take place (30,31). Both mechanisms require the AICDA (32). By immunohistology on paraffin sections, we confirmed in allograft ILFs the presence of Ki-67^+ proliferating cells forming a GC where AICDA is expressed (Figure 5A, right panel). Surprisingly, GCs in allograft ILFs bear an increased number of Ki-67^+ cells and staining intensity is homogenous, which does not allow to discriminate properly between dark and light zones in allograft ILFs as it is seen in non-Tx ILFs (Figure 5A, left panel). We found a similar scenario for $AICDA^+$ B cells, ubiquitous staining in the GC of allograft ILF (Figure 5B, right panel), whereas in non-Tx ILFs $AICDA^+$ cells are clustered densely in the dark zone (Figure 5B, left panel). The higher number of $AICDA^+$ B cells was confirmed by a sevenfold increase of *AICDA* gene expression in allograft compared to non-Tx ILFs (Figure 5C).

Location of follicular helper T cells in isolated lymphoid follicles

From studies in human tonsils, we know that T_{FH} are localized in mature GC expressing high level of the inhibitory co-receptor programmed cell death-1 (PD-1) (33) and around 15–25% of $CXCR5^+$ T_{FH} express CD57 (34). Therefore, we performed immunohistochemistry on paraffin sections with anti-PD-1 and anti-CD57 antibodies to elucidate the presence of PD-1^+ and $CD57^+$ T_{FH} in allograft and non-Tx ILFs. We found PD-1^+ and $CD57^+$ cells in the

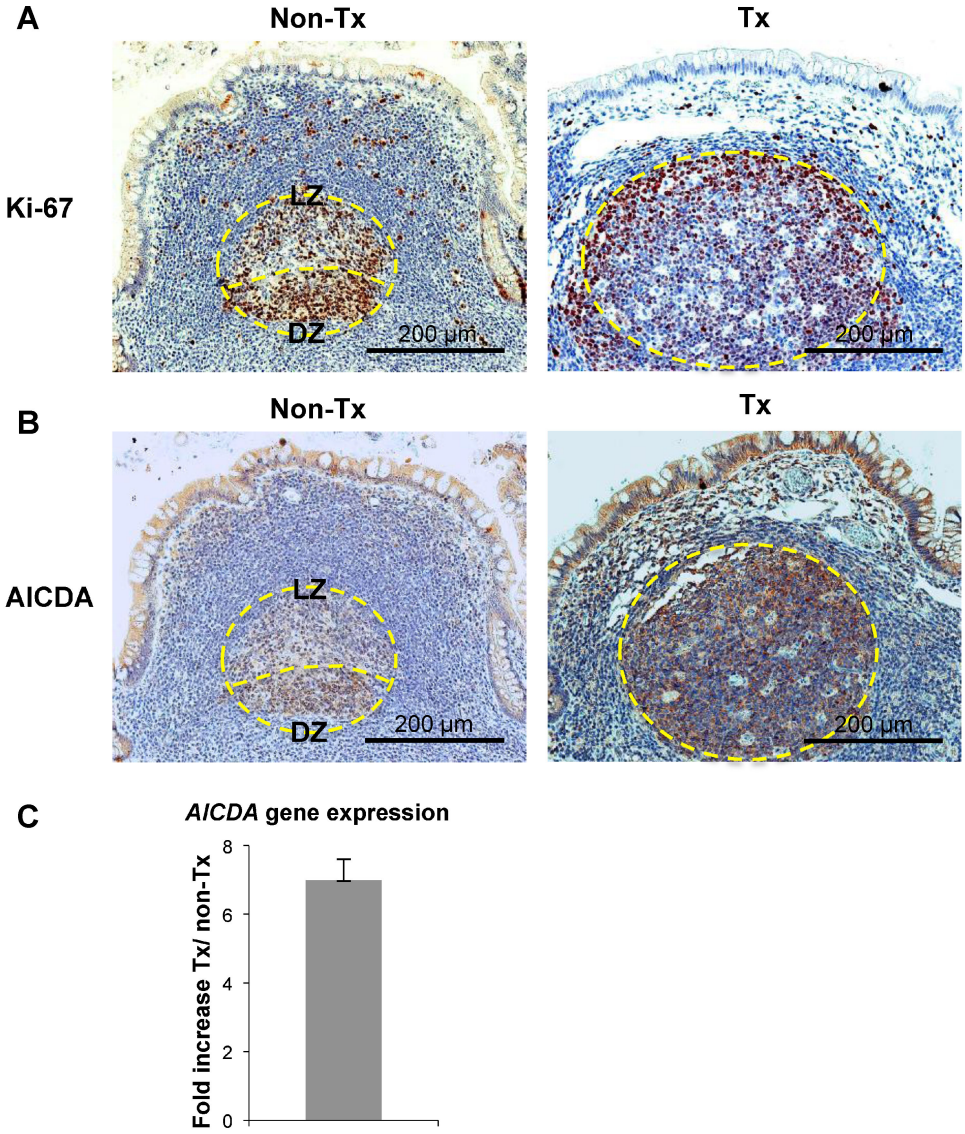

Figure 5: Comparison of germinal center (GC) in allograft ILF and nontransplant (non-Tx) ILF. (A) Paraffin sections of distal ileum stained with Ki-67 proliferation marker. Image shows typical staining pattern with proliferating Ki-67$^+$ centroblasts forming the dark zone (DZ) and viewer Ki-67$^+$ B cells in the light zone (LZ) (left panel). Note the lack of LZ and DZ in the Tx sample (right panel). (B) Immunohistochemical staining with anti-AICDA antibodies on small bowel sections depicting homogeneous AICDA expression throughout allograft GC, whereas in non-Tx GC it is clearly distributed into LZ and DZ. Representative pictures of stainings from eight allograft and six non-Tx tissues. Original magnification 200×. (C) Quantitative real-time polymerase chain reaction analysis showing a sevenfold increase of *AICDA* gene expression in allograft ILFs (n = 4) compared to that in non-Tx ILFs (n = 5). Expressed are mean and SD. AICDA, activation-induced cytidine deaminase; ILF, isolated lymphoid follicle.

GC light zone of all-mature non-Tx and allograft ILFs confirming the presence of T_{FH} in the allograft ILFs (Figure 6).

IgA positive plasma cells in the allograft lamina propria

The output of proper function of follicular structures (inductive site) is IgA-secreting plasma cells in the LP of the gut mucosa, the effector site (15,17). Recently, the critical contribution of ILFs to luminal IgA production has been highlighted in mice (35) and in humans (36). To determine whether IgA$^+$ plasma cells are situated correctly in the allograft LP and cell numbers are similar in the allograft and non-Tx mucosal tissue, we performed immunohistology on paraffin-embedded sections with anti-IgA antibody. In both groups, IgA$^+$ plasma cells could be detected at the middle and lower part of the villus axis (Figure 7A). There was a significantly higher number of IgA$^+$

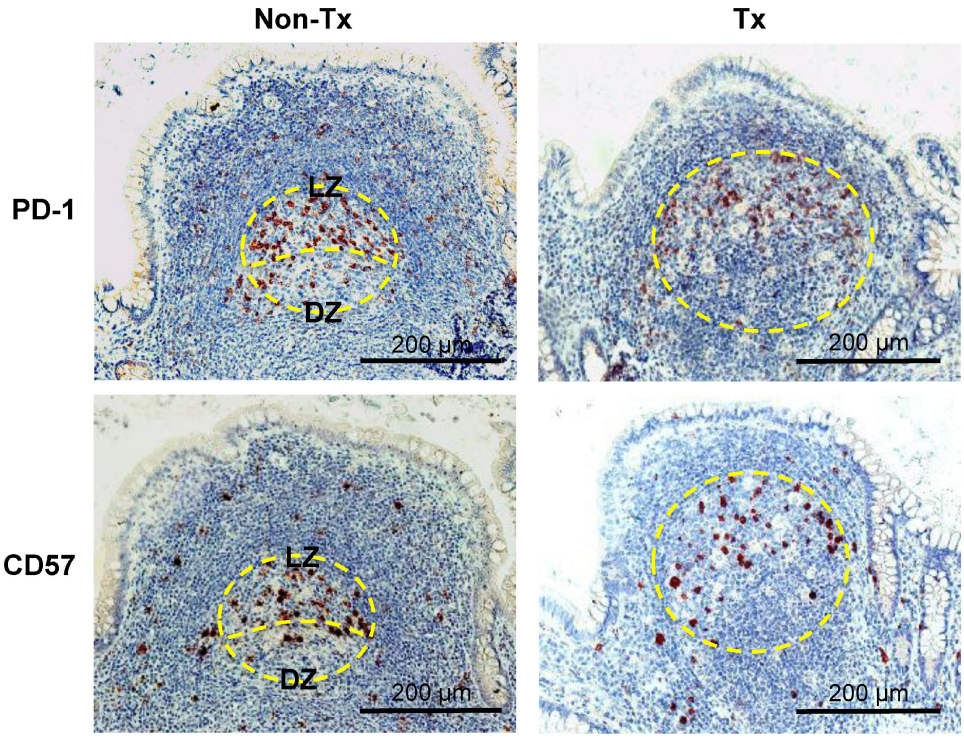

Figure 6: Immunosuppressive regimen does not influence the appearance of CD4$^+$ follicular helper T cells (T_{FH}). Pictures correspond to representative immunohistochemical images with anti-PD-1 and anti-CD57 antibodies. PD-1$^+$ and CD57$^+$ T_{FH} are localized in the light zone (LZ) of the germinal centers from allograft and non-Tx isolated lymphoid follicles. Original magnification 100×. DZ, dark zone; PD-1, programmed cell death-1; Tx, transplant.

plasma cells (32 ± 5.3 cells of eight Tx vs. 24 ± 3.2 cells of six non-Tx samples; $p = 0.0185$) in the allograft than in non-Tx mucosa (Figure 7B).

Discussion

Our results indicate that constitution, integrity and function of allograft ILFs after ITx are not profoundly affected by the chronic immunosuppressive regimen, whereas GCs from allograft ILFs are in a higher proliferation state and the number of IgA$^+$ plasma cells in the allograft LP are increased compared to non-Tx samples.

Moghaddami et al (10) discovered and histologically described ILFs as separate structures from PPs in the human small intestine in 1998. ILFs were then studied separately from PPs in mouse models (37,38), whereas in human studies until now this discrimination was not taken into account and both structures were pooled and analyzed as lymphoid follicles (39,40). We established a technique to accurately distinguish ILF from PP structures by examining the epithelial- and seromuscular-freed mucosa.

Our results show that ILF structures *per se* are in a higher frequency than PPs. We detected ILFs in 95% (18/19) of the obtained specimens (allograft and non-Tx), whereas only 21% (4/19) had one or two PPs. The range of collected ILFs per specimen was between 12 and 130 (mean: 36), which is much higher in number than the reported range 0–10 (mean: 2) ILFs per 2–12 (mean: 6) biopsies per patient by Junker et al (40). The high number of collected ILFs per specimen allowed us to conduct follicular cell analysis by flow cytometry and cell sorting. Beneath the advantage of obtaining an important number of ILFs, ileostomy closure specimens were in this study a minimum of 10 months postoperation under immunosuppressive regimen with tacrolimus, corticosteroids and mycophenolate mofetil.

We confirmed by the STR method that allograft ILFs are repopulated and filled-up with 88.2% of recipient lymphocytes at the time of ileostomy closure demonstrating that follicles are fully functional. We analyzed a biopsy from day 6 post-Tx containing ILF structures and detected that 51% of follicular cells were of recipient origin. This revealed that repopulation of allograft ILFs is taking place early after operation. This is in line with results from a multivisceral Tx rat model where at day 12 post-Tx 50% of PPs were of recipient origin (41).

We further showed by flow cytometry that the main lymphocyte subsets (CD19$^+$ B cells, CD4$^+$ T cells and CD8$^+$ T cells) from allograft ILFs have similar percentages

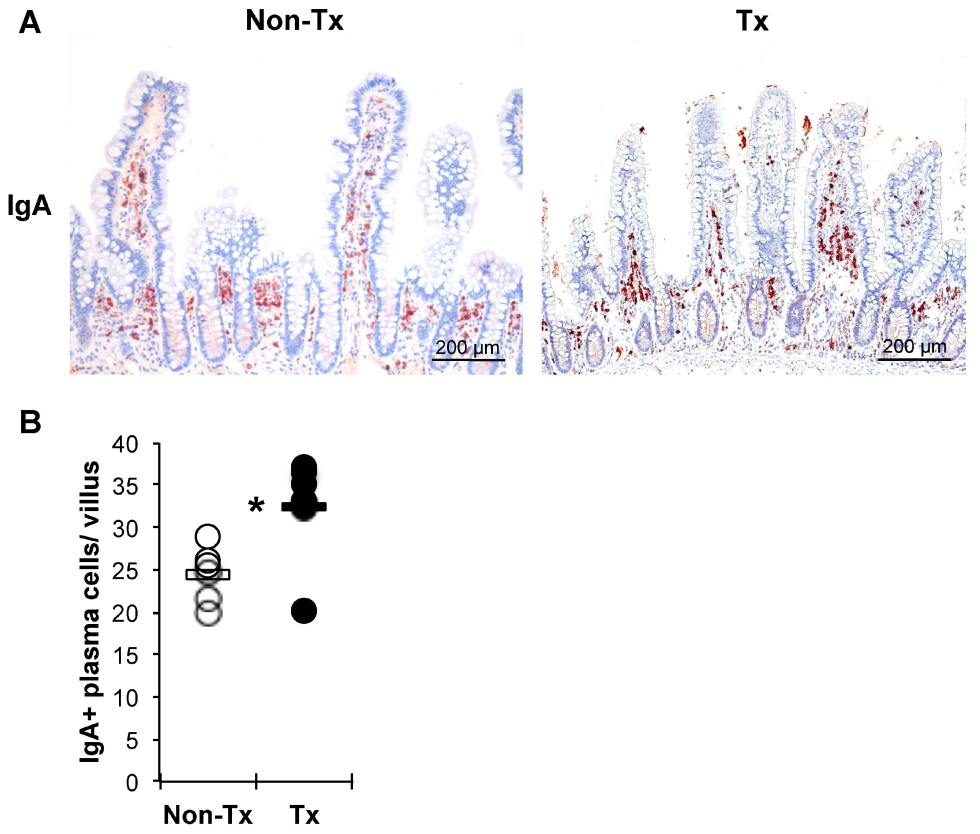

Figure 7: Increased number of IgA$^+$ plasma cells in allograft compared to nontransplant lamina propria (non-Tx LP). (A) Representative pictures of anti-IgA antibody staining of plasma cells in the LP of non-Tx (left panel) and of allograft (right panel) mucosal tissues. (B) IgA$^+$ cells were counted in five villi (each villus with a minimum length of 200 µm) per patient and mean numbers expressed as circles and dots, bars representing mean of each group. * indicates significant differences.

compared to non-Tx ILFs and similar percentages to the results by Junker et al (40) demonstrating that the applied immunosuppressive regimen was not significantly influencing cell composition in the allograft ILFs. We could not detect any correlation between individual cell percentages of allograft ILFs and patients' data, such as age, immunosuppressive regimen or clinical events. Takama et al (42) depicted the capacity of tacrolimus to reduce blood T cells in their ITx rat model, whereas they reported no significant reduction of T cells in allograft PPs. Our findings extend this concept showing that B cell activation in ILF and mucosal IgA production is not affected by the maintenance immunosuppressive regimen applied to the ITx patient.

Mature, active ILF bears GC with a dark zone, where centroblasts undergo SHM, and with a light zone, where centrocytes further differentiate into plasma cells. The dark zone can be clearly discriminated from the light zone by staining with proliferation marker Ki-67 and AICDA, reflecting a higher density of Ki-67$^+$ and AICDA$^+$ cells. We confirmed the presence of Ki-67$^+$ and AICDA$^+$ cells in the allograft ILFs drawing the conclusion that allograft ILFs are functionally active. Strikingly, in allograft ILFs, no clear separation of dark and light zones with the Ki-67 and AICDA markers could be detected and the diameter of GC in the allograft ILFs was enlarged (data not shown) compared to GC of control ILFs. In addition, we calculated a sevenfold increase of *AICDA* mRNA expression in allograft ILFs. Altogether, we conclude that allograft ILFs are hyperplastic or hyperactive compared to non-Tx ILFs. This might be explained by microbiota in the ileostomy revealing a shift from anaerobic to aerobic microorganisms due to oxygen access (43) and, consequently, this change in the commensal community might stimulate ILF maturation. Although more B cells were proliferating, CD4$^+$ and CD8$^+$ T cells showed similar levels of the activation marker CD69 in both allograft and non-Tx ILFs. mRNA of interferon gamma is not expressed higher in Tx versus non-Tx (data not shown), suggesting a noninflammatory state of the allograft ILFs. Although it has been suggested that donor lymphoid organs are the main sites for rejection amplification (44), we could not find any differences in various cell populations of patients that experienced ACR episodes and those with no ACR episodes. Hypertrophic lymphoid follicles with enlarged GCs have been detected in diverse diseases,

such as inflammatory bowel disease, follicular lymphoma, bacterial and parasitic infections, and in nodular lymphoid hyperplasia (45).

Our analysis on $CD4^+$ Th cell subsets confirmed the presence of various subsets within the allograft ILFs. Our results of gene expression analysis revealed that in allograft ILFs $CXCR5^+$ $CD4^+$ T cells express the *BCL6* transcription factor, the cytokine *IL21*, and the chemokine *CXCL13* (data not shown), a typical expression pattern for human T_{FH} that was first reported in the tonsils (13,46). The $CD4^+$ $CCR6^+$ T cell subset expresses typical genes of Th17 cells (*RORC* and *IL17A*) and of Tregs (*FOXP3* and *TGFB*). We also confirmed the presence of T_{FH} by immunohistology with two typical markers, PD-1 (47) and CD57 (34) in allograft ILFs underlining the findings that the applied immunosuppressive regimen has no influence on cell composition of allograft ILFs.

The limitations of this study are the number of patients, the unpredictable ILF number in the ileostomy closure specimen, and the long waiting period for obtaining ileostomy closure samples. Furthermore, the control sample should be the donor tissue specimen obtained at ablation, which is not always applicable. To overcome the restricted number of patients, a close collaboration with other centers should be worthwhile. For the follow-up analysis of follicles, the application of the colorant indigo carmine during endoscopy that better identifies follicles, demonstrated by MacDonald et al (39), might be evaluated.

In summary, we show in this work the feasibility of studying allograft ILFs in the ITx setting. We have demonstrated that in spite of the immunosuppressive regimen used in transplant patients allograft ILFs are still functional. Our results might certainly stimulate future studies about the impact of different immunosuppressive regimen on the mucosal immune system of allograft tissue including the effect of potential local therapies for immune modulation of the intestinal graft.

Acknowledgments

The authors thank Marcela Alvarez for histological preparation of tissue samples. We would like to thank Joe and Katherine Abdo for carefully proofreading our manuscript. This work was supported by grants from *Agencia Nacional de Promoción de la Ciencia y la Tecnología ANPCYT* (PICT 01799) and from the European Union (INCO-CT-2006-032296). GHD, GEG and MR are members of Research Career from Argentinean National Research Council (CONICET).

Disclosure

The authors of this manuscript have no conflicts of interest to disclose as described by the *American Journal of Transplantation*.

References

1. Fishbein TM. Intestinal transplantation. N Engl J Med 2009; 361: 998–1008.
2. Grant D, Abu-Elmagd K, Reyes J, et al. 2003 report of the intestine transplant registry: A new era has dawned. Ann Surg 2005; 241: 607–613.
3. Pabst R, Russell MW, Brandtzaeg P. Tissue distribution of lymphocytes and plasma cells and the role of the gut. Trends Immunol 2008; 29: 206–208, author reply 209–210.
4. Herbrand H, Bernhardt G, Forster R, Pabst O. Dynamics and function of solitary intestinal lymphoid tissue. Crit Rev Immunol 2008; 28: 1–13.
5. Pabst O, Herbrand H, Worbs T, et al. Cryptopatches and isolated lymphoid follicles: Dynamic lymphoid tissues dispensable for the generation of intraepithelial lymphocytes. Eur J Immunol 2005; 35: 98–107.
6. Brandtzaeg P, Kiyono H, Pabst R, Russell MW. Terminology: Nomenclature of mucosa-associated lymphoid tissue. Mucosal Immunol 2008; 1: 31–37.
7. Newberry RD. Intestinal lymphoid tissues: Is variety an asset or a liability? Curr Opin Gastroenterol 2008; 24: 121–128.
8. Newberry RD, Lorenz RG. Organizing a mucosal defense. Immunol Rev 2005; 206: 6–21.
9. Brandtzaeg P, Pabst R. Let's go mucosal: Communication on slippery ground. Trends Immunol 2004; 25: 570–577.
10. Moghaddami M, Cummins A, Mayrhofer G. Lymphocyte-filled villi: Comparison with other lymphoid aggregations in the mucosa of the human small intestine. Gastroenterology 1998; 115: 1414–1425.
11. Cornes JS. Number, size, and distribution of Peyer's patches in the human small intestine: Part I. The development of Peyer's patches. Gut 1965; 6: 225–229.
12. Wang C, McDonald KG, McDonough JS, Newberry RD. Murine isolated lymphoid follicles contain follicular B lymphocytes with a mucosal phenotype. Am J Physiol Gastrointest Liver Physiol 2006; 291: G595–G604.
13. Crotty S. Follicular helper CD4 T cells (TFH). Annu Rev Immunol 2011; 29: 621–663.
14. Glaysher BR, Mabbott NA. Isolated lymphoid follicle maturation induces The development of follicular dendritic cells. Immunology 2007; 120: 336–344.
15. Knoop KA, Newberry RD. Isolated lymphoid follicles are dynamic reservoirs for the induction of intestinal IgA. Front Immunol 2012; 3: 84.
16. Lorenz RG, Newberry RD. Isolated lymphoid follicles can function as sites for induction of mucosal immune responses. Ann N Y Acad Sci 2004; 1029: 44–57.
17. Fagarasan S, Muramatsu M, Suzuki K, Nagaoka H, Hiai H, Honjo T. Critical roles of activation-induced cytidine deaminase in the homeostasis of gut flora. Science 2002; 298: 1424–1427.
18. Hu S, Yang K, Yang J, Li M, Xiong N. Critical roles of chemokine receptor CCR10 in regulating memory IgA responses in intestines. Proc Natl Acad Sci U S A 2011; 108: E1035–E1044.
19. Bouskra D, Brezillon C, Berard M, et al. Lymphoid tissue genesis induced by commensals through NOD1 regulates intestinal homeostasis. Nature 2008; 456: 507–510.
20. Gondolesi G, Fauda M. Technical refinements in small bowel transplantation. Curr Opin Organ Transplant 2008; 13: 259–265.
21. Meier D, Cagnola H, Ramisch D, et al. Analysis of immune cells draining from the abdominal cavity as a novel tool to study intestinal transplant immunobiology. Clin Exp Immunol 2010; 162: 138–145.

22. Ruiz P, Bagni A, Brown R, et al. Histological criteria for the identification of acute cellular rejection in human small bowel allografts: Results of the pathology workshop at the VIII International Small Bowel Transplant Symposium. Transplant Proc 2004; 36: 335–337.
23. Rumbo M, Sierro F, Debard N, Kraehenbuhl JP, Finke D. Lymphotoxin beta receptor signaling induces the chemokine CCL20 in intestinal epithelium. Gastroenterology 2004; 127: 213–223.
24. Cornes JS. Peyer's patches in the human gut. Proc R Soc Med 1965; 58: 716.
25. Van Kruiningen HJ, West AB, Freda BJ, Holmes KA. Distribution of Peyer's patches in the distal ileum. Inflamm Bowel Dis 2002; 8: 180–185.
26. Fazilleau N, Mark L, McHeyzer-Williams LJ, McHeyzer-Williams MG. Follicular helper T cells: Lineage and location. Immunity 2009; 30: 324–335.
27. Heidt S, Roelen DL, Eijsink C, et al. Calcineurin inhibitors affect B cell antibody responses indirectly by interfering with T cell help. Clin Exp Immunol 2010; 159: 199–207.
28. Annunziato F, Cosmi L, Santarlasci V, et al. Phenotypic and functional features of human Th17 cells. J Exp Med 2007; 204: 1849–1861.
29. Sallusto F, Lanzavecchia A. Heterogeneity of CD4+ memory T cells: Functional modules for tailored immunity. Eur J Immunol 2009; 39: 2076–2082.
30. Klein U, Dalla-Favera R. Germinal centres: Role in B-cell physiology and malignancy. Nat Rev Immunol 2008; 8: 22–33.
31. Victora GD, Nussenzweig MC. Germinal centers. Annu Rev Immunol 2012; 30: 429–457.
32. Pavri R, Nussenzweig MC. AID targeting in antibody diversity. Adv Immunol 2011; 110: 1–26.
33. Iwai Y, Okazaki T, Nishimura H, Kawasaki A, Yagita H, Honjo T. Microanatomical localization of PD-1 in human tonsils. Immunol Lett 2002; 83: 215–220.
34. Kim CH, Rott LS, Clark-Lewis I, Campbell DJ, Wu L, Butcher EC. Subspecialization of CXCR5+ T cells: B helper activity is focused in a germinal center-localized subset of CXCR5+ T cells. J Exp Med 2001; 193: 1373–1381.
35. Tsuji M, Suzuki K, Kitamura H, et al. Requirement for lymphoid tissue-inducer cells in isolated follicle formation and T cell-independent immunoglobulin A generation in the gut. Immunity 2008; 29: 261–271.
36. Barone F, Patel P, Sanderson JD, Spencer J. Gut-associated lymphoid tissue contains the molecular machinery to support T-cell-dependent and T-cell-independent class switch recombination. Mucosal Immunol 2009; 2: 495–503.
37. Hamada H, Hiroi T, Nishiyama Y, et al. Identification of multiple isolated lymphoid follicles on the antimesenteric wall of the mouse small intestine. J Immunol 2002; 168: 57–64.
38. Lorenz RG, Chaplin DD, McDonald KG, McDonough JS, Newberry RD. Isolated lymphoid follicle formation is inducible and dependent upon lymphotoxin-sufficient B lymphocytes, lymphotoxin beta receptor, and TNF receptor I function. J Immunol 2003; 170: 5475–5482.
39. MacDonald TT, Spencer J, Viney JL, Williams CB, Walker-Smith JA. Selective biopsy of human Peyer's patches during ileal endoscopy. Gastroenterology 1987; 93: 1356–1362.
40. Junker Y, Bode H, Wahnschaffe U, et al. Comparative analysis of mononuclear cells isolated from mucosal lymphoid follicles of the human ileum and colon. Clin Exp Immunol 2009; 156: 232–237.
41. Murase N, Demetris AJ, Matsuzaki T, et al. Long survival in rats after multivisceral versus isolated small-bowel allotransplantation under FK 506. Surgery 1991; 110: 87–98.
42. Takama Y, Miyagawa S, Yamamoto A, et al. Effects of a calcineurin inhibitor, FK506, and a CCR5/CXCR3 antagonist, TAK-779, in a rat small intestinal transplantation model. Transpl Immunol 2011; 25: 49–55.
43. Hartman AL, Lough DM, Barupal DK, et al. Human gut microbiome adopts an alternative state following small bowel transplantation. Proc Natl Acad Sci U S A 2009; 106: 17187–17192.
44. Wang J, Dong Y, Sun JZ, et al. Donor lymphoid organs are a major site of alloreactive T-cell priming following intestinal transplantation. Am J Transplant 2006; 6: 2563–2571.
45. Kokkonen J, Karttunen TJ. Lymphonodular hyperplasia on the mucosa of the lower gastrointestinal tract in children: An indication of enhanced immune response? J Pediatr Gastroenterol Nutr 2002; 34: 42–46.
46. Kim CH, Lim HW, Kim JR, Rott L, Hillsamer P, Butcher EC. Unique gene expression program of human germinal center T helper cells. Blood 2004; 104: 1952–1960.
47. Wang C, Hillsamer P, Kim CH. Phenotype, effector function, and tissue localization of PD-1-expressing human follicular helper T cell subsets. BMC Immunol 2011; 12: 53.